



ELSEVIER

Journal of Chromatography A, 908 (2001) 179–184

JOURNAL OF
CHROMATOGRAPHY A

www.elsevier.com/locate/chroma

Control method for integrity of continuous beds

Rainer Hahn, Alois Jungbauer*

Institute of Applied Microbiology, University of Agricultural Sciences, Muthgasse 18, A-1190, Vienna, Austria

Abstract

Monoliths are considered to be the latest version of stationary phases for protein chromatography. They are now becoming popular since they exhibit reduced peak broadening due to low mass transfer resistances. A weak point of monoliths may be an inhomogeneous bed, especially when charged groups are present during co-polymerization. This becomes apparent when a protein solution is loaded onto such a monolith. A biphasic breakthrough curve differing from the sigmoidal-shaped one, is observed. Two error functions were used to approximate the breakthrough curve. From these parameters an estimate of the fraction of flow passing through the homogeneously packed part of the bed as well as the inhomogeneously one was derived. This flow pattern was also confirmed by perfusing ferritin through an inhomogeneous monolith and comparing it to an intact one. Electron microscopy and mercury porosimetry did not indicate any abnormalities in the bed. © 2001 Elsevier Science B.V. All rights reserved.

Keywords: Continuous beds; Monolithic columns; Breakthrough curves; Stationary phases, LC; Proteins; Lysozyme

1. Introduction

Continuous stationary phases, the so-called monoliths, are used for a variety of chromatographic separations employing the same principles of action for the adsorption processes as applied in conventional chromatography [1–13]. It has been empirically found out that monolithic chromatography columns can be operated at very high speed without losing separation efficiency. This phenomenon was explained by a more efficient mass transfer of the solute from the mobile phase into the adsorption surface compared to conventional particulate material [7,14]. A significant fraction of the pores is reached by convection instead of diffusion [15]. Monoliths were cast either from organic copolymers [1,10,16–18] or by agglomeration processes of par-

ticles consisting of inorganic material such as silica or zirconia [12,13,19–22].

The copolymers of glycidyl methacrylate and ethylene glycol dimethacrylate were described by Kubin et al. [23] in the early 1970s. They were used for preparation of conventional particles [24] and later for casting of monoliths [25]. A problem during polymerization is heat dissipation, leading to an inhomogeneous monolith or even worse to cracks within the monolith. This problem has meanwhile been solved, and monoliths are now on the market under the trade names CIM-disk and CIM tube exhibiting excellent flow properties. Whenever copolymerization of a monomer with a charged copolymer was performed, we observed an aberrant breakthrough curve.

Mercury porosimetry was frequently used to measure the pore size and pore size distribution of porous chromatography particles. The method was also successfully applied to measure the pore size distribution of monoliths [18]. Currently it is unclear,

*Corresponding author. Tel.: +43-1-36006-6226; fax: +43-1-36006-1249.

E-mail address: jungbaue@hp01.boku.ac.at (A. Jungbauer).

if such a method is capable to measure the integrity of monoliths. Josic et al. [26] proposed a method to inspect the integrity of monoliths by perfusing them with ferritin. Flow abnormalities or inhomogeneous distribution over the monolith caused by the flow distributor could be simply visualized. After cutting the monolith the internal flow pattern could also be made visible. Unfortunately the ferritin-method and the mercury porosimetry are not nondestructive analytical methods. Thus, both described methods are not suitable for rapid analysis and quality control; especially when individual columns should be tested. Therefore, there is a demand for the development of nondestructive methods for the analysis of integrity of monoliths.

Upon loading a column until breakthrough, a sigmoidal breakthrough curve can be observed. This curve can be approximated by various models such as described by Thomas [27], Lapidus and Amundsen [28] and Rosen [29]. Independent of the model and the assumption made, the breakthrough curve has a sigmoidal shape, when a single solute is fed to the column. Deviations from the sigmoidal shape could be interpreted as flow abnormalities within a monolith assuming that all other contributions to the chromatographic process are working properly. In the presented work we investigated prototype monoliths with an aberrant breakthrough curve and correlated this behavior to results obtained by the ferritin method or by mercury porosimetry.

2. Theory

For description of the breakthrough curve (BTC) of a damaged monolith an empirical approach was developed. From the approximation of the breakthrough curve by an additive cumulative Gaussian function, the ratio of flow passing through the part with internal cracks or inhomogeneities as well as through the intact bed should be accessible. A bed containing a crack was virtually segregated into two beds of different sizes.

The total flow (F_{total}) is diverted into a flow through the crack (F_{crack})¹ and a flow through the

intact bed (F_{bed}). Both virtual beds have a certain adsorption capacity, although the adsorption capacity of the crack is much lower.

The hold up time of the bed is

$$\hat{t}_{\text{bed}} = \frac{V_{\text{bed}}}{F_{\text{bed}}} \quad (1)$$

and the hold up time of the crack is

$$\hat{t}_{\text{crack}} = \frac{V_{\text{crack}}}{F_{\text{crack}}} \quad (2)$$

while $\hat{t}_{\text{crack}} < \hat{t}_{\text{bed}}$.

The biphasic BTC was described by an additive cumulative Gaussian function (the error function)

$$C = \text{erf}(a, b, c) + \text{erf}(d, e, f) + g \quad (3)$$

where C is the column outlet concentration, b describes the residence time of the protein in the crack; c is the zone width (shock layer thickness) and a the amplitude.

The amplitude corresponds to

$$a - g = C \cdot \frac{F_{\text{crack}}}{F_{\text{total}}} \quad (4)$$

The behavior of the intact bed is characterized by the second error function, where e describes the residence time, f the zone width and d the amplitude of the BTC of the intact bed. The amplitude corresponds to

$$d - g = C \cdot \frac{F_{\text{bed}}}{F_{\text{total}}} \quad (5)$$

Parameter g describes the baseline. Upon attaining equilibrium in both beds, the column outlet concentration (C_{outlet}) equals the feed concentration C_0 .

$$C_{\text{outlet}} = C_0 \cdot \frac{F_{\text{crack}}}{F_{\text{bed}} + F_{\text{crack}}} + C_0 \cdot \frac{F_{\text{bed}}}{F_{\text{bed}} + F_{\text{crack}}} \quad (6)$$

The first part of Eq. (6) is proportional to a and the second part to d .

$$a - g = C_0 \cdot \frac{F_{\text{crack}}}{F_{\text{bed}} + F_{\text{crack}}} \quad (7)$$

$$d - g = C_0 \cdot \frac{F_{\text{bed}}}{F_{\text{bed}} + F_{\text{crack}}} \quad (8)$$

From Eqs. (7) and (8) the ratio of flow between the intact bed and the crack can be estimated.

¹Here we denote a crack as a part of the column having a different packing density than the rest. It does not have to be a crack in the common meaning.

3. Experimental

3.1. Chromatography

Determination of breakthrough curves was performed as follows. Monoliths were put in a cartridge as shown by Josic and Strancar [8] and connected to a fast protein liquid chromatography (FPLC) system equipped with UV monitor. UV signals were continuously monitored and signals were electronically stored and for data processing converted to an ASCII file.

Lysozyme was used as model protein solution. The protein was dissolved in a 20 mM Tris buffer, pH 8.0. Protein was then loaded until the column outlet concentration approximated the feed concentration. The velocity applied was 200 cm/h corresponding to a flow-rate of 4 ml/min.

3.2. Monoliths

Polymethacrylate-based monoliths were produced by copolymerization of glycidyl methacrylate and ethylene diglycol methacrylate as described by Tenikova et al. [25]. It was attempted to incorporate charged ligands into the polymerization mixture. The cast monolith had a diameter of 1.2 cm and a height of 0.3 cm.

3.3. Visualization of the flow distribution

A method described by Josic et al. [30] was applied to visualize the unequal (inhomogeneous) flow distribution. Ferritin (2 mg/ml) was dissolved in a 20 mM Tris buffer, pH 8.0, and subsequently loaded until a significant contrast could be observed at the bottom of the disk.

3.4. Mercury porosimetry

Dried monoliths were immersed in liquid mercury. The volume of the intruded mercury is a direct measure for the penetrated pore volume. The experiments were performed on a mercury porosimeter Pascal 440 (ThermoQuest Italia, Rodano, Italy).

3.5. Electron microscopy

Scanning electron microscopy (SEM) was performed with a DSM 990 digital scanning electron micrograph from Zeiss (Oberkochen, Germany).

4. Results and discussion

Incorporation of charged groups during polymerization would increase the possibilities to form novel and unique adsorption surfaces with the benefit of fast mass transfer properties unique for monoliths.

Whenever we tried to copolymerize in presence of charged monomers, we observed an aberrant BTC of the generated monolith. This was not observed with commercially available monoliths. It was not clear, whether cracks and cavities were generated or zones within the monolith with different packing densities of the agglomerated particles. As a result of the irregular bed, the breakthrough curve diverged from the expected sigmoidal form.

In Fig. 1 an electron micrograph of such a monolith is shown in different magnifications. At the beginning of the study the incapability of this destructive method to rapidly detect an inhomogeneous distribution of the pore-forming material or cracks was not apparent, although the specimen was analyzed very carefully at different orientations and

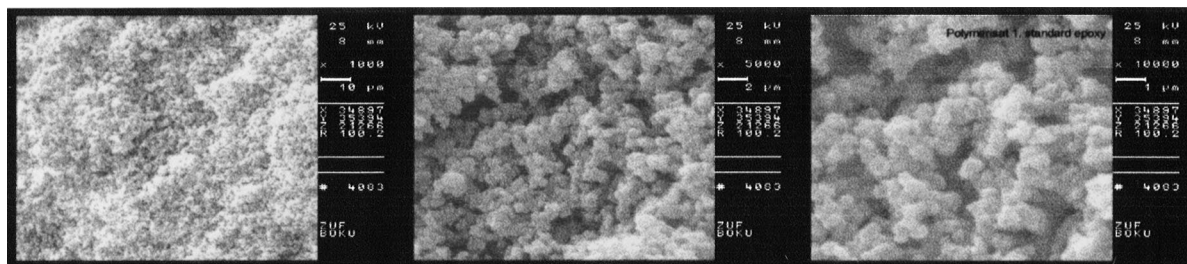


Fig. 1. SEM of monoliths produced by copolymerization of glycidylmethacrylate and ethylene glycol dimethacrylate.

depths of the block. Only a small part of the monolith can be scanned therefore not being representative for the entire block. Another explanation is that the structural differences responsible for the flow abnormalities cannot be made visible by this technique. In Fig. 2 the breakthrough curves of an intact monolith and monoliths with potential inhomogeneous distributions of the continuous beds are shown. For monoliths with the aberrant breakthrough behavior a biphasic curve was observed. In all cases the monoliths were placed into the same column holder, ensuring that the extra-column contributions cannot be made responsible for this aberrant breakthrough curve. For further investigations of the flow behavior of the monolith, the columns were perfused with a ferritin solution as described in the ex-

perimental section. Ferritin binds unspecifically to the polymethacrylate support. In zones where the flow is preferred more ferritin was bound per time compared to zones with lower flow. By the adsorption of ferritin, a brownish-colored protein, one can easily distinguish zones with different flows. The intact zone cannot be physically discriminated from the “damaged” one, only a difference can be made visible. Cavities in the particle-agglomerates cause maldistribution of flow resulting in a more intensely colored zone. If the maldistribution is caused by packing differences, it could be either the less intensely colored zone or the darker one. An example of an intact monolith with a sigmoidal breakthrough curve is shown in Fig. 2A. For this experiment we have used a commercially available CIM-disk. Homogeneous distribution of ferritin can be observed at the bottom of the disk (Fig. 3A). Investigating monoliths with a biphasic breakthrough curve (Fig. 2B), the “ferritin-method” indicated an inhomogeneous distribution of the flow over the superficial area of the disk at the bottom side (Fig. 3B). Another example of maldistribution of the solutes within the monolith is shown in Fig. 3C indicating that a crack might be present. The small spot is interpreted as a physical crack and fast flow through the cavity produced the dark spot.

The breakthrough curve of the prototype monolith was approximated by Eq. (3). The estimated parameters are listed in Table 1. Inserting these parameters in Eqs. (7) and (8) yielded the ratio of flow through both zones of the monolith; the intact one and the one with maldistribution of flow. In this example the total flow was 4 ml/min, and the flow through the

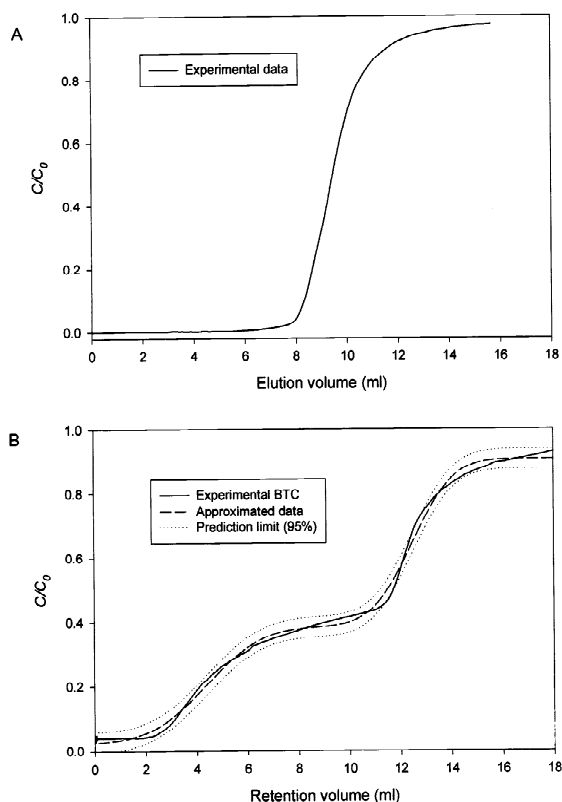


Fig. 2. Breakthrough curves observed when loading a single solute onto (A) a commercially available intact disk, and (B) a prototype disk synthesized with a charged copolymer exhibiting aberrant flow properties.

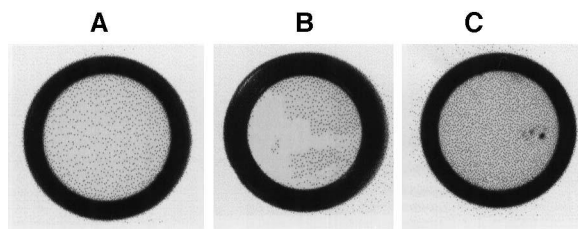


Fig. 3. Photograph of the column outlet after perfusion with ferritin. (A) Commercially available intact disk, (B) prototype disk synthesized with a charged copolymer exhibiting aberrant flow properties and (C) disk damaged by a very small crack.

Table 1
Summary of information derived by approximation of biphasic breakthrough curve with Eq. (3)

Parameters Eq. (1)	Estimated values
<i>a</i>	0.36
<i>b</i>	4.38
<i>c</i>	1.74
<i>d</i>	0.52
<i>e</i>	12.46
<i>f</i>	1.28
<i>g</i>	0.02

irregular zone was 1.6 ml/min. These values match nicely with the areas of the flow distribution made visible by the ferritin-method.

The intact and the prototype monoliths were also examined by mercury porosimetry. The pore size distributions are shown in Fig. 4. A significant difference could not be detected. One would expect a bimodal pore size distribution originating from the zone with low and high packing density.

It is evident that the breakthrough curve is very sensitive to irregularities in a monolithic column. A pulse experiment performed with a damaged monolith results just in a slight shift in retention time and peak broadening. Frontal loading accumulates the deviation of normal shape.

Further studies will be necessary to completely understand the flow in a monolith. NMR is certainly one of the preferred techniques. Also analytical tools

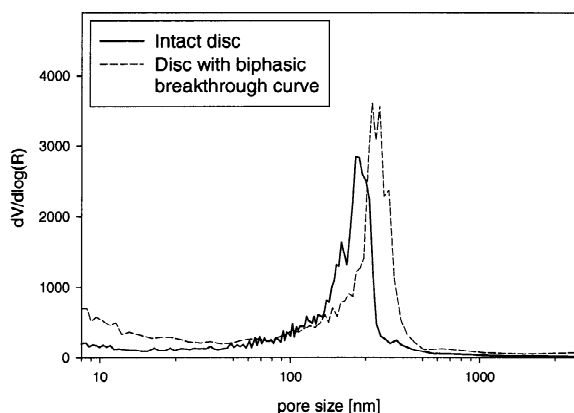


Fig. 4. Pore size distribution obtained by mercury porosimetry.

must be developed to gain an insight into the connectivity and tortuosity of the pores.

Acknowledgements

The work has been carried out within the EUREKA project FAST1. This project has been enabled by a grant from the “Österreichischer Forschungsförderungsfonds der gewerblichen Wirtschaft” and by the support of the company OCTAPHARMA. The SEM was performed by M. Sara and C. Mader at the Center of Ultrastructural Research of the University of Agricultural Sciences, Vienna. We also want to acknowledge the helpful discussion and the support of the company BIA Separations.

References

- [1] S. Hjerten, J. Liao, R. Zhang, *J. Chromatogr.* 473 (1989) 273.
- [2] J.L. Manganaro, B.S. Goldberg, *Biotechnol. Prog.* 9 (1993) 285.
- [3] Y.M. Li, J.L. Liao, K. Nakazato, J. Mohammad, L. Terenius, S. Hjertén, *Anal. Biochem.* 223 (1994) 153.
- [4] J.L. Liao, C.M. Zeng, A. Palm, S. Hjerten, *Anal. Biochem.* 241 (1996) 195.
- [5] J.L. Liao, Y.M. Li, S. Hjerten, *Anal. Biochem.* 234 (1996) 27.
- [6] R. Giovannini, R. Freitag, T.B. Tennikova, *Anal. Chem.* 70 (1998) 3348.
- [7] G. Iberer, R. Hahn, A. Jungbauer, *LC-GC* 17 (1999) 998.
- [8] D. Josic, A. Strancar, *Ind. Eng. Chem. Res.* 38 (1999) 333.
- [9] A. Podgornik, M. Barut, J. Janca, A. Strancar, T. Tennikova, *Anal. Chem.* 71 (1999) 2986.
- [10] F. Svec, J.M. Frechet, *Ind. Eng. Chem. Res.* 38 (1999) 34.
- [11] K. Amatschek, R. Necina, R. Hahn, E. Schallaun, H. Schwinn, D. Josic, A. Jungbauer, *J. High Resolut. Chromatogr.* 23 (2000) 47.
- [12] K. Cabrera, D. Lubda, H. Eggenweiler, H. Minakichi, K. Nakanishi, *J. High Resolut. Chromatogr.* 23 (2000) 93.
- [13] M. Schulte, D. Lubda, A. Delp, *J. High. Resolut. Chromatogr.* 23 (2000) 100.
- [14] R. Hahn, A. Jungbauer, *Anal. Chem.* (2000) in press.
- [15] J.J. Meyers, A.I. Liapis, *J. Chromatogr. A* 852 (1999) 3.
- [16] S. Hjerten, M. Li, J. Mohammed, K. Nakazato, G. Pettersson, *Nature* 356 (1992) 810.
- [17] A. Strancar, M. Barut, A. Podgornik, P. Koselj, D. Josic, A. Buchacher, *LC-GC Int.* October (1998) 1.
- [18] M.B. Tennikov, N.V. Gazdina, T.B. Tennikova, F. Svec, *J. Chromatogr. A* 798 (1998) 55.

- [19] S.M. Fields, *Anal. Chem.* 68 (1996) 2709.
- [20] K. Cabera, G. Wieland, D. Lubda, K. Nakanishi, N. Soga, H. Minakuchi, K. Unger, *Trends Anal. Chem.* 1 (1998) 50.
- [21] N. Ishizuka, H. Minakuchi, N. Najanishi, N. Soga, J. Tanaka, *J. High Resolution Chromatogr.* 21 (1998) 477.
- [22] H. Kobayashi, H. Nagayama, T. Ikegami, K. Hosoya, J. Tanaka, *Chromatographia* 20 (1999) 166.
- [23] M. Kubin, P. Spacek, R. Chromecek, *Collect. Czech. Chem. Commun.* 32 (1967) 3881.
- [24] T.B. Tennikova, D. Horák, F. Svec, J. Kolár, J. Coupek, S.A. Trushin, V.G. Maltzev, B.G. Belenkii, *J. Chromatogr.* 435 (1988) 357.
- [25] T. Tennikova, F. Svec, B.G. Belenkii, *J. Liq. Chromatogr.* 13 (1990) 63.
- [26] D. Josic, J. Reusch, K. Loster, O. Baum, W. Reutter, *J. Chromatogr.* 590 (1992) 59.
- [27] H.C. Thomas, *J. Am. Chem. Soc.* 66 (1944) 1664.
- [28] L. Lapidus, N.R. Amundson, *J. Phys. Chem.* 56 (1952) 984.
- [29] J. Rosen, *J. Chem. Phys.* 20 (1952) 387.
- [30] D. Josic, Y.P. Lim, A. Strancar, W. Reutter, *J. Chromatogr. B.* 662 (1994) 217.